Article:
Baqer, Y orcid.org/0000-0002-1195-8797, Chen, X orcid.org/0000-0002-2053-2448, Rochelle, C et al. (1 more author) (2020) Modelling of multi-minerals kinetic evolution in hyper-alkaline leachate for a 15-year experiment. Environmental Science and Pollution Research, 27. pp. 35604-35617. ISSN 0944-1344

https://doi.org/10.1007/s11356-020-09875-x

Modelling of multi-minerals kinetic evolution in hyper-alkaline leachate for a 15-year experiment

Yousef Baqer[1], XiaoHui Chen[1]*, Christopher Rochelle[2], Steven Thornton[3]

School of Civil Engineering, University of Leeds, LS2 9JT

[1]*School of Civil Engineering, University of Leeds.

Telephone: +44 (0)113 3430350

Email: x.chen@leeds.ac.uk

[2] British Geological Survey

[3] Groundwater Protection and Restoration Group, Dept of Civil and Structural Engineering, The University of Sheffield

Abstract

Cement has been widely used for low- to intermediate-level radioactive waste management; however, the long-term modelling of multiple mineral transfer between the cement leachate and the host rock of a geological disposal facility remains a challenge due to the strong physical-chemical interactions within the chemically-disturbed zone. This paper presents a modelling study for a 15-year experiment simulating the reaction of crystalline basement rock with evolved near-field groundwater (pH = 10.8). A mixed kinetic equilibrium (MKE) modelling approach was employed to study the dolomite-rich fracture-filling assemblage reacting with intermediate cement leachate. The study found that the mineralogical and geochemical transformation of the system was driven by the kinetically-controlled dissolution of the primary minerals (dolomite, calcite, quartz, k-feldspar and muscovite). The initial high concentration of calcium ions appeared to be the main driving force initiating the dedolomitization process, which played a significant role in the precipitation of secondary talc, brucite and Mg-aluminosilicate minerals. The modelling study also showed that most of the initially precipitated calcium silicon hydrate phases redissolved and formed more stable calcium silicon aluminium hydrate phases. The findings highlight the importance of a deep and insightful understanding of the geochemical transformations based on the type and characteristics of the host rock, where the system is under out of equilibrium conditions, and the rates of mineral reactions.

Keywords: Cement, Radioactive waste disposal, Mineral evolution, Modelling, Cement leachate, Alkaline fluids, PHREEQC

1. Introduction

Underground geological facilities are the most secure places to store/dispose of radioactive wastes generated during the civil/military programmes, and also generated through scientific, engineering and medical usage. One concept for low- and intermediate-level radioactive waste involves constructing an underground facility in a host rock at a depth of several hundred metres, then backfilling with a cementitious material. Such a facility is designed to achieve two main safety objectives: 1) to isolate the radioactive waste from the biosphere, and 2) to provide multiple barriers (including a high pH environment) to minimise radionuclide mobility over long timescales.

The containment system involves multiple barriers in which the engineered barriers work alongside natural ones (e.g. stable and low permeability host rock) to prevent the release of radionuclides to the biosphere. The concept has been adopted by several countries, including the UK, Sweden and South Korea (Authority 2010a; Francis et al. 1997; Kim et al. 2007; Skogsberg and Ingvarsson 2006). The final design and performance assessment of the engineered barrier can be influenced by the waste inventory, the surrounding conditions that can be expected during the performance assessment timescale and the degree of reaction with the surrounding host geology. Usually, the near field plays a crucial role in providing long-term control over radionuclide migration, which limits their release to the surrounding environment. Over time, the chemical properties (e.g., sorption capacity, reactive surface area) and physical properties (e.g., porosity, permeability) of the host rock in the near field barrier evolve as a result of the interactions with their surroundings and with other barriers. As this will happen long before any potential migration

of radionuclides, it is useful to understand and to be able to predict these changes, as they are likely to influence potential radionuclide retardation.

One of the challenges in evaluating the effectiveness of an engineered barrier is understanding the extent to which the evolving process of the near field host rock may occur. This will help in assuring that the engineered barrier materials will fulfil their safety functions over performance assessment timescales. The evolution of near field properties will strongly be linked to the interaction of the host rock and high pH water leaching out of the cement (the 'alkaline disturbed zone', ADZ).

Cement leachate is usually formed when the facility is closed and becomes saturated with groundwater that then reacts and equilibrates with the cementitious engineered barrier. The reaction process results in a high-pH plume that inhibits corrosion and limits some radionuclide solubility. Eventually, some cement leachate will migrate into the surrounding rock and create a chemically disturbed zone (CDZ) at the interface between the cement barrier and the host rock, initiating a series of reactions (Chen et al. 2016; Chen and Thornton 2018; Chen et al. 2015). The dissolution of primary minerals in the host rock is likely to be accompanied by precipitation of new minerals with evolved chemical and physical properties that may contribute to decreased radionuclide mobility through processes such as the reduction in permeability, increased sorption, and coprecipitation.

For a cement-based geological disposal facility, several experimental studies and numerical models have been performed to demonstrate the reaction of highly-alkaline cement leachate with

minerals in the host rock (Berner 1990; Harris et al. 2001a; Harris et al. 2001b; Schwyn et al. 2003). Previous research has considered three cement leachate evolution stages based on the progression of pH values (Small et al. 2016), which can be summarised as: young cement leachate (YCL), intermediate cement leachate (ICL) and old cement leachate (OCL). The reaction of ICL with the near field host rock is the focus of this study, and this may result in the formation of a changing series of mineral assemblages, changes to mineral surfaces, variations in pH, as well as other changes (Moyce et al. 2014). These processes will eventually affect the sorption capability of radionuclides at the mineral surface (Authority 2010b).

The paper models mineral evolution in a 15-year laboratory experiment, analysing interlinks among multiple minerals known to occur in Borrowdale Volcanic Group (BVG) rocks in reaction with ICL (the BVG is an important basement rock in north-west England, and which was previously investigated by UK Nirex Limited (Francis et al. 1997). Importantly, the rock sample comprised a hydraulically-conductive dolomite-rich fracture, and thought dolomite is only a minor phase in the rock overall; it is a major phase in direct contact with current groundwater. The modelling process implements the concept of a mixed kinetic equilibrium approach (MKE), which combines the advantages of both equilibrium and kinetic formulations to enable the modelling of complex geochemical reactions (Bethke 1994; Bethke 1996; Chen and Thornton 2018; Van der Lee 1997; Van der Lee 1998; Westall 1986). This approach was initially developed to overcome the shortage of kinetic data for minerals that dissolve and precipitate (Soetaert et al. 1996), assuming a faster reaction by means of the equilibrium concept and a slower reaction controlled by the kinetic process (Atkinson et al. 1988; Hoch et al. 2012). The model is used to develop a

deeper understanding of the pH evolution along with quantification of the amount of host rock minerals dissolving or precipitating in the near field/alkaline disturbed zone.

2. Experimental study

The experiment was conducted by the British Geological Survey (Moyce et al. 2014; Rochelle et al. 2016; Rochelle et al. 1997) over the course of 15 years, starting in 1995, and being part of a larger series of experiments of different durations. The original intent of the experiment was to study the reaction of a sample of Ordovician age Borrowdale Volcanic Group (BVG) rock with both a pH 13 'young near-field porewater' (YNFP) and a pH 12 'evolved near-field groundwater' (ENFG) (rock type and fluid naming convention based on that used in the Nirex Safety Assessment research programme [NSARP] at the time). These fluids represent, respectively, 'young cement leachate (YCL) and 'intermediate cement leachate' (ICL) (naming convention used in the BIGRAD project) released from a representative cementitious barrier that could be used in a deep geological disposal facility for intermediate-level radioactive waste. Although the experiments significantly exceeded their originally planned durations and also that of the NSARP, it was useful to continue them as the BVG contains many mineral phases typical of crystalline basement rocks in general. In the experiment of relevance to the study presented here, a dolomite-rich fracture assemblage in the BVG was reacted with YNFP, and the resultant solid and fluid products initially examined after 15 months and also for up to 15 years. The focus of the current study was to better understand the mineralogical evolution of this experimental system for the entire 15 years, in order to investigate longer-term geochemical processes.

Figure 1: Stainless steel pressure vessels lined with Teflon® used to contain the BVG and synthetic CDZ-type fluid experiments.

Two PTFE-lined stainless steel vessels, of 150 mL and 100 mL, were used for the 'reacting' and blank experiments, respectively (Figure 1). The solid phase consisted of a piece of drill core containing altered wall rock and a dolomite-rich fracture fill from a hydrogeological conductive fracture zone in the BVG. The 2-kg rock sample was then disaggregated and sieved (Moyce et al. 2014; Rochelle et al. 1997). In the 'reacting' experiment, 35 g of disaggregated BVG was used with 140 g of groundwater-cement leachate, and the stainless-steel vessel was kept in a 70°C oven. The smaller blank experiment just contained the leachate. The ENFG leachate was presented by slightly saline water (Na/CaCl) saturated with $Ca(OH)_2$ (Table 1). All preparation processes were performed under a nitrogen atmosphere to prevent reaction of the alkaline water with atmospheric carbon dioxide. During the reaction, the rock underwent mineralogical changes that changed the concentration of the dissolved ions in the ENFG leachate. Experiments were terminated and sampled after the fourth, ninth and fifteenth months (Rochelle et al. 2016; Rochelle et al. 1997), and importantly also at the end of the fifteenth year (Moyce et al. 2014). The solid experimental residues were washed in propan-2-ol and then dried prior to storage and analysis. For X-ray diffraction analysis, a subsample was milled and a 10% corundum (Al_2O_3) standard added. A diffractometer instrument (PANalytical X'Pert Pro) with PANalytical X'Pert Highscore Plus

152 software was then used to carry out the final mineralogical analysis (Moyce et al. 2014; Rochelle
153 et al. 2016).
154
155 Table 1: Composition of the Evolved Near-Field Groundwater (ENFG) prepared by the British Geological Survey
156 (Rochelle et al. 2016; Rochelle et al. 1997).

Chemical component	Concentration (mg/L)
Al	4.17
B	0.335
Ba	0.017
Br	23.2
CO_3	20
Ca	1930
Cl	15100
F	0.03
Fe	0.120
K	185
Li	0.153
Mg	0.117
Mn	0.010
Na	9160
SO_4	1090
NO_3	20
Si	2.07
Sr	166
pH (at 70ºC)	10.84

157
158 ***3. Modelling methodology***
159
160 The conceptual model developed for this study is presented in Figure 2. The idea was developed
161 based on theoretical and experimental analysis. The MKE approach is based upon the timescale of
162 each mineral reaction rate (i.e., which reaction is faster and which slower). For each mineral, either
163 a kinetic or equilibrium approach, or a mix of both (if the difference between rates was more than
164 10^2), was used to provide the supporting information for the software. The concept of MKE has
165 been widely implemented in subsurface geochemical applications, as it allows both kinetic and

equilibrium reactions to model a multiphase and multi-component system (Brun and Engesgaard 2002; Lichtner 1996; Mayer et al. 2002; Prommer et al. 2003).

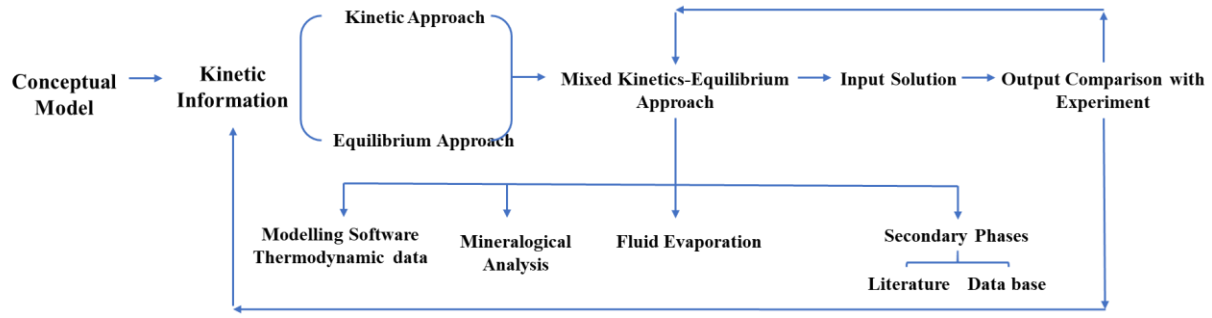

Figure 2: Conceptual Model for the Mixed Kinetic-Equilibrium approach.

3.1. Conceptual model software and thermodynamic data

The simulation carried out in this study was performed with the PHREEQC code (version 3.6.1). The software can compute a wide range of chemical reactions in aqueous geochemical systems, utilising both chemical thermodynamic and kinetic data. In recent years, several databases have been developed by various authors to optimise the use of this geochemical code. For a cement leachate–host rock reaction in an underground repository, the Lawrence Livermore National Laboratory (LLNL), Thermoddem, Thermoddem DB and CEMDATA DB databases were applied by previous researchers (Blanc et al. 2012; Lothenbach et al. 2019; Wolery 1992; Wolery and Daveler 1992). In this work, LLNL database (Delany and Lundeen 1990) –was utilise though with some modifications, namely; the addition of kinetic information for calcium silicon hydrate (CSH) and calcium silicon aluminium hydrate phases (CASH). This database seemed to be the best option available since it has kinetic information for a variety of minerals and aqueous species, especially carbonate minerals that are required for the simulation of phases present in the BVG rock sample. The data of thermodynamic reactions (equilibrium constants) for the major minerals are shown in

Table 2 (Chen and Thornton 2018). Note that the below values of $log\, K_{eq}$ are valid for the experiment condition.

Table 2: Reactions and equilibrium constants for minerals used in the calculations.

Mineral	*Reaction*	*Log Keq*
Calcite	$CaCO_3 + H^+ = Ca^{++} + HCO_3^-$	*1.8487*
Muscovite	$KAl_3Si_3O_{10}(OH)_2 + 10H^+ = K^+ + 3Al^{+++} + 3SiO_2 + 6H_2O$	*13.5858*
Kaolinite	$Al_2Si_2O_5(OH)_4 + 6H^+ = +2Al^{+++} + 2SiO_2 + 5H_2O$	*6.8101*
Quartz	$SiO_2 = +1.0\ SiO_2$	*-3.9993*
Dolomite	$CaMg(CO_3)_2 + 2H^+ = +1.0Ca^{++} + 1.0\ Mg^{++} + 2\ HCO_3^-$	*2.5135*
K-feldspar	*KAlSi3O8 +4.0000 H+ = + 1.0000 Al+++ + 1.0000 K+ + 2.0000 H2O + 3.0000 SiO2*	*-0.2753*
Brucite	$Mg(OH)_2 + 2H^+ = +1.0\ Mg^{++} + 2H_2O$	*16.2980*
Tobermorite-11A	$Ca_5Si_6H_{11}O_{22.5} + 10H^+ = +5Ca^{++} + 6SiO_2 + 10.5H_2O$	*65.6121*
Saponite-Mg	*Mg3.165Al.33Si3.67O10(OH)2 +7.3200 H+ = + 0.3300 Al+++ + 3.1650 Mg++ + 3.6700 SiO2 + 4.6600 H2O*	*26.2523*
Nontronite-Mg	*Mg.165Fe2Al.33Si3.67H2O12 +7.3200 H+ = + 0.1650 Mg++ + 0.3300 Al+++ + 2.0000 Fe+++ + 3.6700 SiO2 + 4.6600 H2O*	*-11.6200*
Talc	*Mg3Si4O10(OH)2 +6.0000 H+ = + 3.0000 Mg++ + 4.0000 H2O + 4.0000 SiO2*	*21.1383*
Mesolite (Zeolite)	*Na.676Ca.657Al1.99Si3.01O10:2.647H2O +7.9600 H+ = + 0.6570 Ca++ + 0.6760 Na+ + 1.9900 Al+++ + 3.0100 SiO2 + 6.6270 H2O*	*13.6191*
Stilbite (Zeolite)	*Ca1.019Na.136K.006Al2.18Si6.82O18:7.33H2O +8.7200 H+ = + 0.0060 K+ + 0.1360 Na+ + 1.0190 Ca++ + 2.1800 Al+++ + 6.8200 SiO2 + 11.6900 H2O*	*1.0545*

3.2. Mineralogical analysis and kinetic information

The mineralogical composition of the BVG rock used in the experiment is shown in Table 3. The concept of MKE was applied to the minerals existing in the rock that react with the ENFG leachate. The initial mass of each reactant was calculated based upon its abundance in the 35 g BVG sample (Rochelle et al. 2016; Rochelle et al. 1997). Note that the original rock sample showed some traces of other fracture filling phases such as clays, but these were not included in the model.

Table 3: BVG rock sample composition. Analysis conducted by the British Geological Survey (Rochelle et al. 2016; Rochelle et al. 1997). The mass of each phase (m_0) is calculated based on a 35g rock sample.

Mineral	Weight %	m_0 (g)
Orthoclase	12	4.2
Quartz	41	14.35
Dolomite	29	10.15
Muscovite	13	4.55
Hematite	2	0.7
Calcite	3	1.05

When cement leachate encounters the surrounding host rock, they will be out of chemical equilibrium, and local dissolution of existing 'primary' minerals will occur. The process releases new solutes into the reaction system, resulting in the precipitation of new 'secondary' minerals. Some secondary phases can have enhanced sorption and permeability-limiting properties relative to the primary phases, and are thus beneficial in term of limiting radionuclide migration. Thus it is important to be able to describe/model the temporal evolution of these phases.

Commonly, the rate of mineral dissolution is measured experimentally by measuring the rate of change in solute concentration as a function of time under 'far from equilibrium' conditions. To model the experimental values of dissolution and precipitation, a variety of factors must first be addressed, which include: the reactive surface area of the mineral, initial and final amounts, the specific dissolution rate constant, and slowing of reaction as equilibrium is approached. The availability of these data is one of the challenges in the field of modelling mineral dissolution and precipitation. The MKE approach is implemented to overcome that drawback with a proper representation of the geochemical system. Equation 1 is a general form that is usually used to calculate the overall dissolution rate of minerals (Appelo and Postma 2005; Parkhurst and Appelo 1999; Rimstidt and Barnes 1980).

$$\boldsymbol{R_k = r_k \frac{A_0}{V}\left(\frac{m_k}{m_{0k}}\right)^n} \quad (1)$$

where

$$\boldsymbol{r_k = k_k\left(1 - \left(\frac{IAP}{K}\right)_k\right)} \quad (2)$$

R is the overall dissolution rate into solution (mol L^{-1} s^{-1}), k_k is the specific dissolution rate (mol/m^2/s), A_0 is the initial surface area (m^2), V is the solution volume (L), m is the moles at a given time and m_0 is the initial moles. $(m_k/m_{0k})^n$ is an interpretation of the changes in the reactive surface area as a result of changes in the size of the mineral during the dissolution process. The value of $n = 2/3$ (Appelo and Postma 2005). (IAP/K) (i.e., ion activity divided by equilibrium constant) is equal to the saturation ratio *(SR)* of the reactant.

It is worth noting that clay minerals were not the focus of the original experiment, and that the exact mica/clay phase(s) present in the fracture of the BVG rock were not fully identified (Moyce et al. 2014). However, muscovite was chosen to represent this phase(s) in the modelling process to control aluminium concentration in solution. Table 4 shows the kinetic information (reaction rate constant, reactive surface area, solution volume) obtained from the literature for the minerals in BVG that were modelled by the MKE approach (k-feldspar, quartz, dolomite, calcite, muscovite). Conversely, hematite was modelled by the equilibrium approach only, because of its low percentage in the rock sample (2%) and its assumed minimal influence on the mineralogical evolution process. In terms of the precipitation process, for most minerals the kinetics and specific rates of precipitation are unknown. Therefore, the precipitation of secondary phases was modelled assuming control by thermodynamic equilibrium.

Table 4: Modelling parameters for the BVG rock. MKE (mixed kinetic equilibrium)

Mineral	Modelling	Solution Volume (L)	Surface area (m^2/g)	Rate constant ($mol\ m^{-2}\ s^{-1}$)
Orthoclase	MKE	0.14 (Rochelle et al. 2016)	0.02 (De Windt et al. 2008)	*k* (using equation 5) (Appelo and Postma 2005)
Quartz	MKE		0.02 (De Windt et al. 2008)	$k = 1x10^{-12.2}$ (70°C) (Worley 1994)
Dolomite	MKE		0.02 (De Windt et al. 2008)	$k= 1.2x10^{-12}$ (Appelo and Postma 2005) This value was lowered two orders of magnitude ($k= 1.2x10^{-10}$)
Muscovite	MKE		1.1 (Knauss 1989)	$k=10^{-18.1}$ (Knauss 1989)
Calcite	MKE		0.02 (De Windt et al. 2008)	*k1 = 10^(0.198 - 444.0 / (273.16 + T))* *k2 = 10^(2.84 - 2177.0 / (273.16 + T))* *k3 = 10^(-1.1 - 1737.0 / (273.16 + T))* in which T denotes temperature. (Appelo and Postma 2005; Plummer et al. 1978)
Hematite	Equilibrium	-	-	-

1) *Quartz* (SiO_2)

As per equation (1) and (2), the overall dissolution kinetic equation for quartz will be:

$$R_{Quartz} = k_{Quartz}\left(\frac{A_0}{V}\right)\left(\frac{m}{m_0}\right)^{0.67}\left(1-\left(\frac{IAP}{K}\right)_{Quartz}\right) \qquad (3)$$

2) *K-feldspar* ($KAlSi_3O_8$)

The overall dissolution rate proposed by (Appelo and Postma 2005; Parkhurst and Appelo 1999) is used to simulate k-feldspar reaction at specific temperatures and pH value:

$$R_{K-feldspar} = k_{K-feldspar}\left(\frac{A_0}{V}\right)\left(\frac{m}{m_0}\right)^{0.67}\left(1-\left(\frac{IAP}{K}\right)_{K-feldspar}\right) \qquad (4)$$

where

$$k_{K-feldspar} = k_{H^+}\frac{[H^+]^n}{f_H} + k_{H_2O}\frac{1}{f_{H_2O}} + k_{OH^-}\frac{[OH^-]^o}{f_{OH}} + k_{CO_2}\frac{[P_{CO_2}]^{0.6}}{f_{CO_2}} \qquad (5)$$

where $k_{K-feldspar}$ is the specific reaction rate (mol m^{-2} s^{-1}), k_i are the solute rate coefficients (mol m^{-2} s^{-1}), and f_i are inhibition factors.

3) *Calcite* ($CaCO_3$)

The specific dissolution rate for calcite was described by (Appelo and Postma 2005; Parkhurst and Appelo 1999; Plummer et al. 1978):

$$r_{calcite} = \left[k_1[H^+] + k_2[H_2CO_3] + k_3[H_2O]\right] * \left[1 - \left(\frac{IAP}{K}\right)^{\frac{2}{3}}_{Calcite}\right] \quad (6)$$

from equation (1), the overall dissolution rate of calcite will then be:

$$R_{calcite} = r_{calcite} \left(\frac{A_0}{V}\right)\left(\frac{m}{m_0}\right)^{0.67} \quad (7)$$

The value of the coefficients k_1, k_2 and k_3 in equations (6) are calculated by (Plummer et al. 1978) by fitting them to the experimental data as a function of temperature.

4) *Dolomite* [$CaMg(CO_3)_2$]

The specific dissolution rate of dolomite is described below by (Appelo et al. 1984; Appelo and Postma 2005; Parkhurst and Appelo 1999).

$$r_{Dolomite} = -k_{Dolomite}\ log\left(\frac{IAP}{K}\right)_{Dolomite} \quad (8)$$

then, the overall dissolution rate of dolomite will be:

$$R_{Dolomite} = r_{Dolomite} \left(\frac{A_0}{V}\right)\left(\frac{m}{m_0}\right)^{0.67} \quad (9)$$

5) *Muscovite* $[KAl_2(AlSi_3O_{10})(OH)_2]$

The specific dissolution rate for muscovite was calculated from the below equation, which was described by (Knauss 1989):

$$r_{Muscovite} = 10^{-18.1}[a_{H^+}]^{+0.22} \quad (10)$$

then, as per equation (1), the overall dissolution rate of muscovite will be:

$$R_{Muscovite} = r_{Muscovite}\left(\frac{A_0}{V}\right)\left(\frac{m}{m_0}\right)^{0.67} \quad (11)$$

3.3.Fluid evaporation

Over the 15-year experiment period, (Rochelle et al. 2016; Rochelle et al. 1997) note that some of the reacting fluid was lost, most likely through diffusion around the threads in the steel vessel. Measures were not taken to limit this process, because the experiments were only initially planned to only run for <18 months. The extent of this process could be estimated based on measured increases in the concentration of conservative (i.e. inactive) dissolved ions in the experiment. In both ENFG experiments (blank and reactive), the chloride ion was set as the inactive and conservative species over the entire experiment period. It was observed that the rate of change in chloride ion concentration was the same in both solutions, and amounted to a 34% fluid loss (Moyce et al. 2014). It is crucial that modelling includes this fluid loss since this loss affects the concentration value (usually measured in mg/L) of all the ions released into the solution. In the modelling procedure, the simulated result of the chloride ion concentration indicated only a 22% fluid loss.

3.4.Secondary phases

During the reaction period of 15 years, the chemical characteristics of the system would significantly evolve and result in multiple cycles of mineral dissolution and precipitation reactions. The type of precipitated secondary mineral can vary over the entire experimental period. In this study, two time periods were defined: from 0 to 15 months (short-term mineral evolution) and from 15 months to 15 years (long-term mineral evolution). In numerical simulations, the specification of each expected secondary mineral was defined to allow its precipitation after saturation. In the modelling process, attention was paid to minerals that were actually observed in the experiments, together with ones that might precipitate (i.e. with saturation index close to zero), in order to achieve more accurate results. Moreover, the list of secondary minerals being tracked during the modelling should reasonably embrace the range of chemical ions represented in the experiment. Finally, the stability range of realistic secondary phases being modelled should be coincident with the experimental conditions (e.g. especially temperature and pH).

Several previous experimental studies have shown that when high-pH calcium-bearing cement leachate reacts with the host rock in the CDZ, the primary silicate dissolves, followed mostly by the precipitation of secondary CSH phases with different calcium-to-silicon ratios (Bateman et al. 1999; Braney et al. 1993; Gaucher and Blanc 2006; Hodgkinson and Hughes 1999; Mäder et al. 2006; Savage and Rochelle 1993). Where the system also includes aluminosilicate minerals (Equations 12 and 13) and potassium (from minerals or the cement leachate), then secondary phases of aluminium- and potassium-bearing minerals (C-[Al]-[K]-S-H) also precipitate (Braney et al. 1993; Savage et al. 1992). Carbonate minerals, especially dolomite, can also play a significant role in the precipitation of other, secondary carbonates (e.g., calcite, Equation 14) when reacting

with cement porewater leachate (Braithwaite and Heath 2013; Poole and Sotiropoulos 1980). Their relatively fast dissolution reaction compared to silicate minerals can control fluid chemistry during the early stages of the reaction (Bérubé et al. 1990; Choquette et al. 1991). Modelling studies have also shown that the reaction time and the composition of the primary solution (e.g., pH) are the two dominant factors in controlling the precipitating phases. Those studies also indicate that over time, CSH gel will evolve into zeolite, feldspar and CSH minerals (Bateman et al. 1999; Braney et al. 1993; Fernández et al. 2010; Pfingsten et al. 2006; Savage et al. 1992; Savage and Rochelle 1993; Soler and Mäder 2007).

$$KAlSi_3O_8 + 3OH^- + 2H_2O \rightarrow Al(OH)_4^- + 3HSiO_{3\,(aq)}^- + K^+{}_{(aq)} \quad (12)$$

$$HSiO_{3\,(aq)}^- + Ca^{2+}{}_{(aq)} + H_2O \rightarrow C-S-H_{gel} \quad (13)$$

$$MgCa(CO_3)_2 + 2OH^- \rightarrow Mg(OH)_2 + CaCO_3 + CO_{3\,(aq)}^{2-} \quad (14)$$

As the BVG rock sample was rich in dolomite, it was assumed that the dedolomitization process would result in an enormous number of magnesium and carbonate ions. This indicates that aqueous calcium ions can also be a driving force for the dissolution process of dolomite, as well as the fluid pH level. At the beginning of the experiments (from 0 to 15 months), there was a low concentration of calcium ions in the YNFP, which led to undersaturation with respect to calcite and its dissolution. However, in the ENFG fluid, the system had a high concentration of calcium ions, which consumed all the aqueous ions of carbonate (CO_3^{2-}) to form the secondary calcite. Since the rock sample also included quartz and feldspar, the released magnesium ions were expected to react with both aqueous calcium and silica to form a secondary (Ca)-Mg-(Al)-(K)-silicate and ettringite (In case sulphate ions were in the solution), as demonstrated in the literature (Derkowski et al. 2013; Galí et al. 2001; Garcia et al. 2020; Schwarzenbach et al. 2013; Techer et al. 2012; Tinseau et al. 2006; Xie et al. 2013). Studies have also confirmed the formation of talc, smectite

(Mg-saponite), illite and brucite as secondary Mg-rich phases during the dedolomitization process (Chen et al. 2018; Moyce et al. 2014; Rochelle et al. 2016). Figure 3 shows the conceptual model for mineral evolution during the dissolution and precipitation cycle of BVG rock reaction with ENFG fluid.

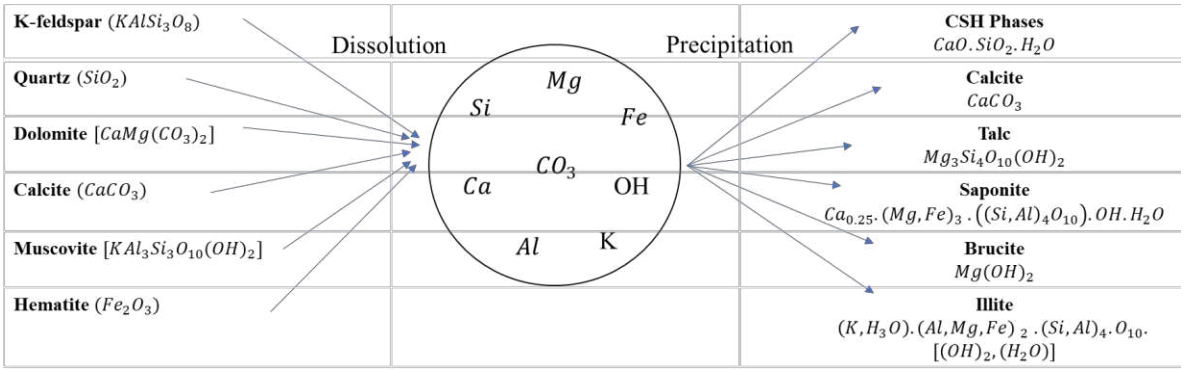

Figure 3: Conceptual model for minerals evolution during the dissolution and precipitation cycle of BVG reaction with ENFG.

4. Results and discussion

The reaction of BVG rock with ENFG was modelled over a simulated 15-year duration using the MKE approach. Changes in the concentration of Ca, Mg, Na, K, Al, Si, CO_3 and pH, as measured from the experiment, were analysed in the modelling simulations, and the comparison is shown in Figures 4–8. As an inactive ion, the chloride concentration (Figure 4, Plot A) increased in the solution as a result of the evaporation process, in line with the experimental data. Furthermore, since none of the primary minerals in the original rock sample included sodium and the potential secondary phases did not significantly consume sodium, the increase in sodium concentration (Plot A) also appears to be mainly a result of the evaporation process. This indicates that the sodium ion is also a conservative species in this geochemical system.

373 The dissolution process of quartz, which accounts for 41% of the BVG rock, released a significant
374 amount of silicon into the highly alkaline solution in the first few months (Plot B). The availability
375 of silicon ions along with the initial calcium concentration (plus calcium released from the
376 dissolution of dolomite) then promoted the precipitation of secondary CSH and CASH phases,
377 represented by a sharp drop in silicon concentration along with a decrease in calcium concentration
378 (Plot C). The increase in potassium concentration (Plot D) was mostly linked to the evaporation
379 plus the dissolution of k-feldspar and muscovite, which also released silicon and aluminium. This
380 can be seen in the numerical results of Plot E, which show a small increase in aluminium
381 concentration in the first few months. The concentration line then drops heavily and follows the
382 experimental behaviour as a result of forming secondary aluminosilicate phases. The saturation
383 index lines in Figure 5 show that k-feldspar and muscovite both start with a higher dissolution rate
384 than quartz, which defines the small peak in aluminium concentration in the beginning before it
385 drops down as secondary calcium silicates start to precipitate. The figure also shows that muscovite
386 was always undersaturated, and thus would have continued to dissolve, providing a source of
387 aluminium for secondary phases. Moreover, the precipitation rates for talc, CSH gel and
388 tobermorite (CSH) were all high in the first few months of the reaction (Figure 7). This high
389 precipitation was mirrored by a substantial drop in silicon, aluminium and calcium concentrations
390 at almost the same time. Note that in Figure 7, the positive value is for the dissolving process,
391 whereas, negative for the precipitation process. Both CSH gel and tobermorite precipitated initially
392 and redissolved after 18 months, with a similar kinetic rate. Talc started to precipitate from the
393 beginning of the experiment and reached a stable amount after around 18 months. The initial
394 concentration of magnesium in the leachate, plus that released during dedolomitization, drove
395 brucite precipitation in the high pH conditions and created a sink for Mg (Bérubé et al. 1990;

Cheng 1986), which also consumed hydroxyl ions and reduced the pH value. This rapid drop in pH in the first few months (Figure 4, Plot H) is also reflected in Figure 6, which shows a higher precipitation rate of brucite in the same period. Subsequently, the drop in the pH value progressively continued, but at a slower rate. From Figure 4 (Plot F), it is also clear that the initial magnesium ions were consumed in the first few months before the dedolomitization process took control. The saturation index of dolomite (Figure 5) shows that it was undersaturated (dissolving) in the geochemical system, but with a much slower rate as the pH value went below 9. This agrees with literature information (Min and Mingshu 1993), which suggests that dedolomitization does not occur below pH 11. Despite that, dedolomitization still occurred in the geochemical system, but at a very slow rate. This is demonstrated by the high magnesium concentration (Evaporation can also play a part in this increase as well) at the end of the 15 years (Figure 4, Plot F), which was observed in the experiment as well (Moyce et al. 2014). The escalation of dedolomitization can be caused by the high concentration of Ca^{2+} in the ENFG, which promotes this process even at lower pH values. Dedolomitization provides calcium and aqueous CO_3^{2-}, which are removed effectively (Figure 4, Plot G) from the system by the precipitation of calcite (Bérubé et al. 1990). This can be seen in the saturation indices of calcite and brucite (Figure 6), which both precipitate in concurrence with the consumption of CO_3^{2-}. The extra amount of CO_3^{2-} in Equation 14 plus the amount released from the dissolution of calcite at later stages of the experiment is also reflected in Figure 4 (Plot G) which shows a small increase in (CO_3^{2-}) concentration. Thus, to incorporate the slow dedolomitization process in the modelling, the specific dissolution rate of dolomite was lowered by two orders of magnitude. This compensates for the slower dolomitisation process below pH 11 but at the same time allows the process to take place, driven by the high concentration of calcium ions, especially at the early stage of the reaction. Another indication that supports the

dedolomitization process is the high precipitation rate of Mg-silicate (talc and saponite-Mg), which was reflected by the higher dissolution rate of dolomite in the same period. Since brucite was close to saturation after the first few months (Figure 6), most of the released magnesium from the dedolomitization process was likely consumed during the formation of magnesium-silicate minerals, which is also recognised in other literature (Eglinton 1998; Glasser 2001).

After the large drop in the pH value, tobermorite and CSH gel starts to dissolve; at that time, a substitution between aluminium and silicon ions takes place to produce more stable calcium aluminosilicate hydrate (Myers et al. 2015; Richardson 2014; Richardson et al. 1993). This secondary CASH phase can then bind with the magnesium from the dedolomitization and create Mg-aluminosilicate (Galí et al. 2001; Moyce et al. 2014). This phenomenon highlights the importance of the modelling procedure for this kind of complex long-term geochemical reaction, as it allows a better understanding of the potential chemical and physical reactions that occur in the geosphere. It can also allow the extension of the timescale from relatively short-duration lab tests to the long timescales of performance assessments. Additionally, it can reveal the type of dissolved or precipitated secondary minerals that can contribute effectively to the retardation of radionuclide migration. For example, zeolites would be useful secondary phases as they have a high sorption capability to the radionuclide. Their considerable surface area and ion exchange capacity could play a key role in retarding radionuclide migration. Unfortunately, no evidence of zeolite precipitation was found in any of the NSARP experiments (Moyce et al. 2014; Rochelle et al. 2016). A plausible explanation for this is the rapid removal of silicon and aluminium by CSH and CASH phases that could suppress the formation of zeolites as they may have slower kinetic precipitation. Even though the modelling results obtained from the geochemical analysis showed

potential for mesolite, stilbite and scolecite precipitation (based on the temperature of the experiment), which all are part of the zeolite family (Figure 8; (Bucher and Stober 2010; Bucher and Weisenberger 2013; Fridriksson et al. 1999; Weisenberger and Selbekk 2009)).

Even though those minerals did not precipitate in the experiment, this does not prove that the situation will be the same in the actual geosphere. The experimental design tried to mimic the actual environmental conditions as much as possible (rock type, temp, pH, etc.). However, there are still some variances, which can lead to different results. For example, as reported by (Adler et al. 1999), zeolite formation is preferred in the pore spaces in which leachate flux is minimal, and in these experiments the leachate: rock ratio was very high. The composition and nature of the rock type can also play a significant role, as it can affect the amount of CO_2 released into the leachate (e.g., depending on dolomite percentage), which can buffer the formation of zeolites (Mullis et al. 1994; Weisenberger and Bucher 2010). Taken together, the findings reveal the potentially important role of dolomite in the geochemical system. Moreover, they provide valuable insight into specific geochemical processes alongside the usefulness of iterating between modelling and experimental results to achieve a better understanding of the system under study.

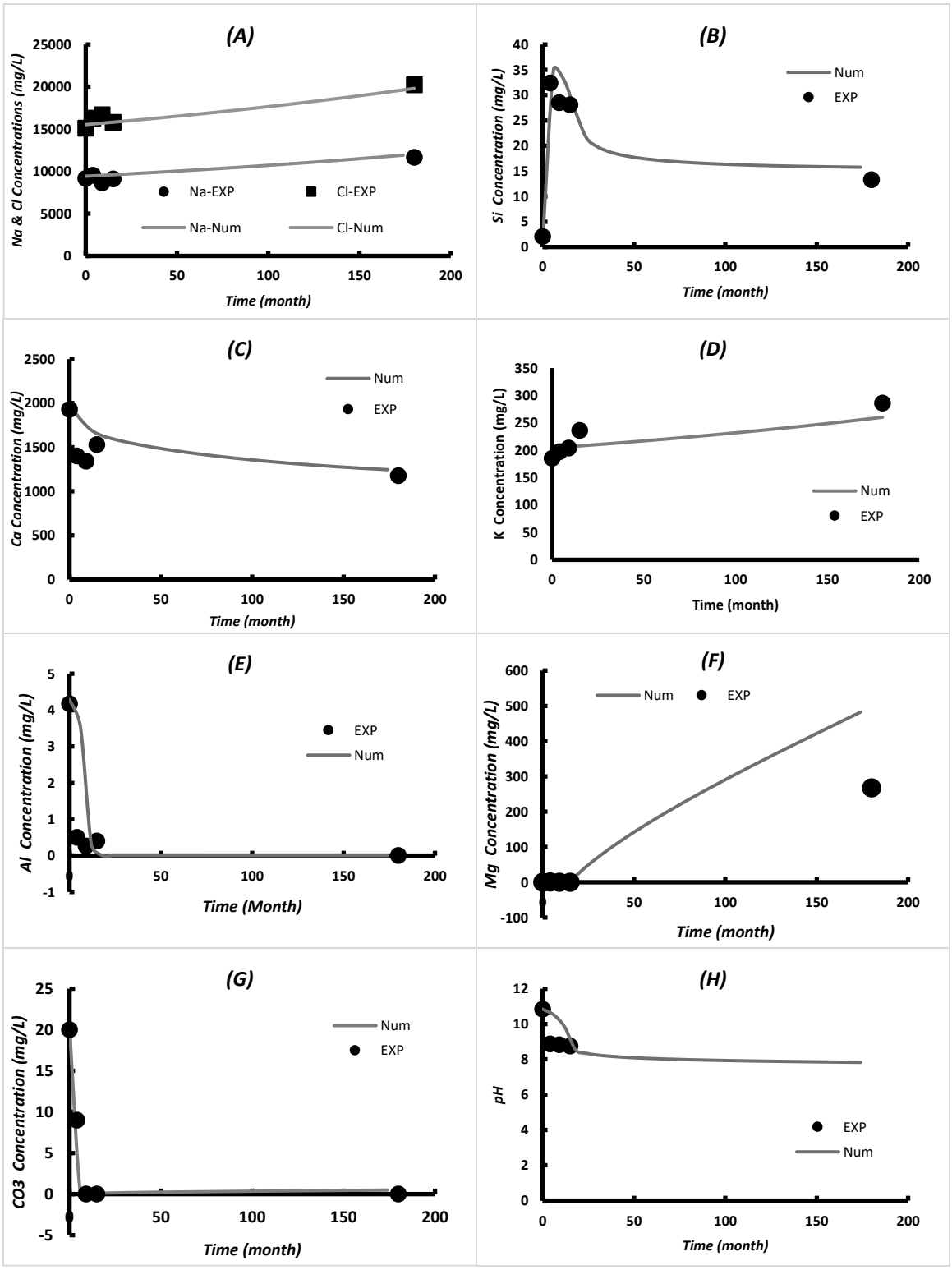

Figure 4: Modelled and experimental values for ions concentration and pH versus time.

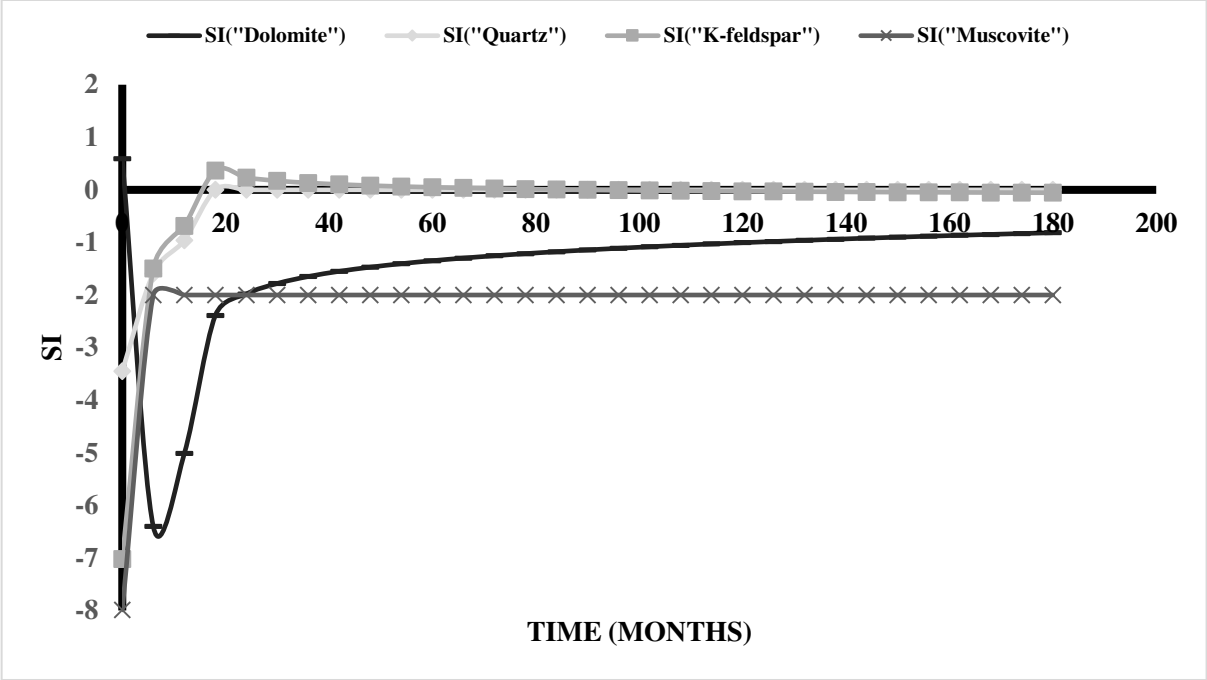

Figure 5: Saturation indices of primary mineral versus time.

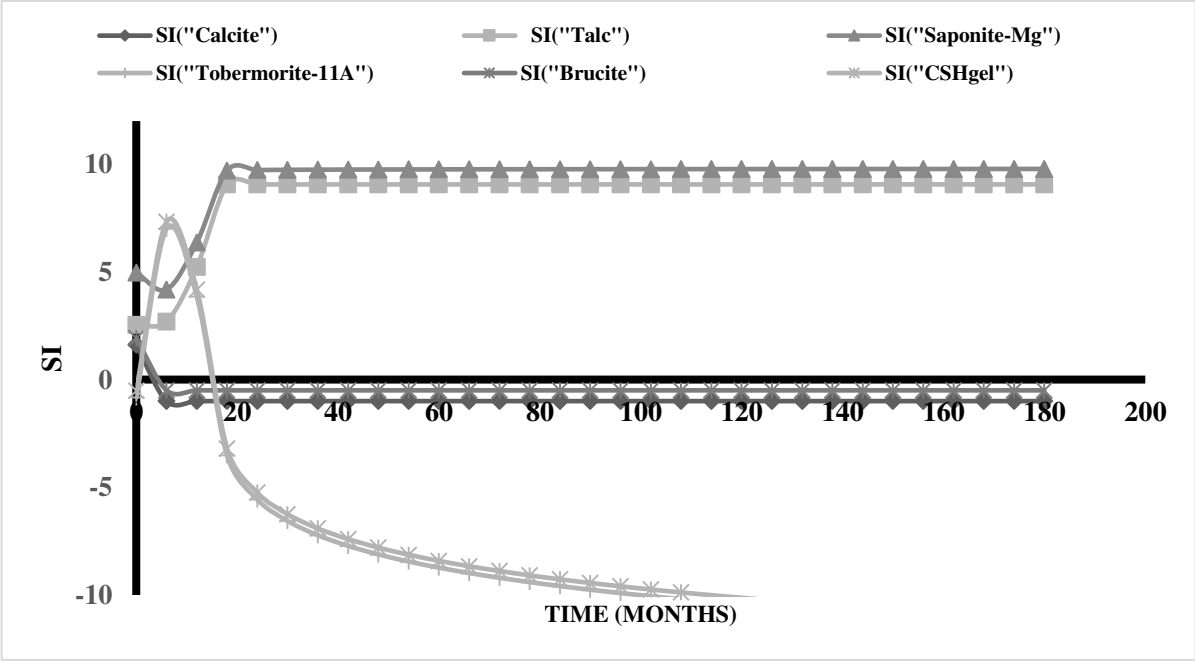

Figure 6: Saturation indices of secondary phases versus time.

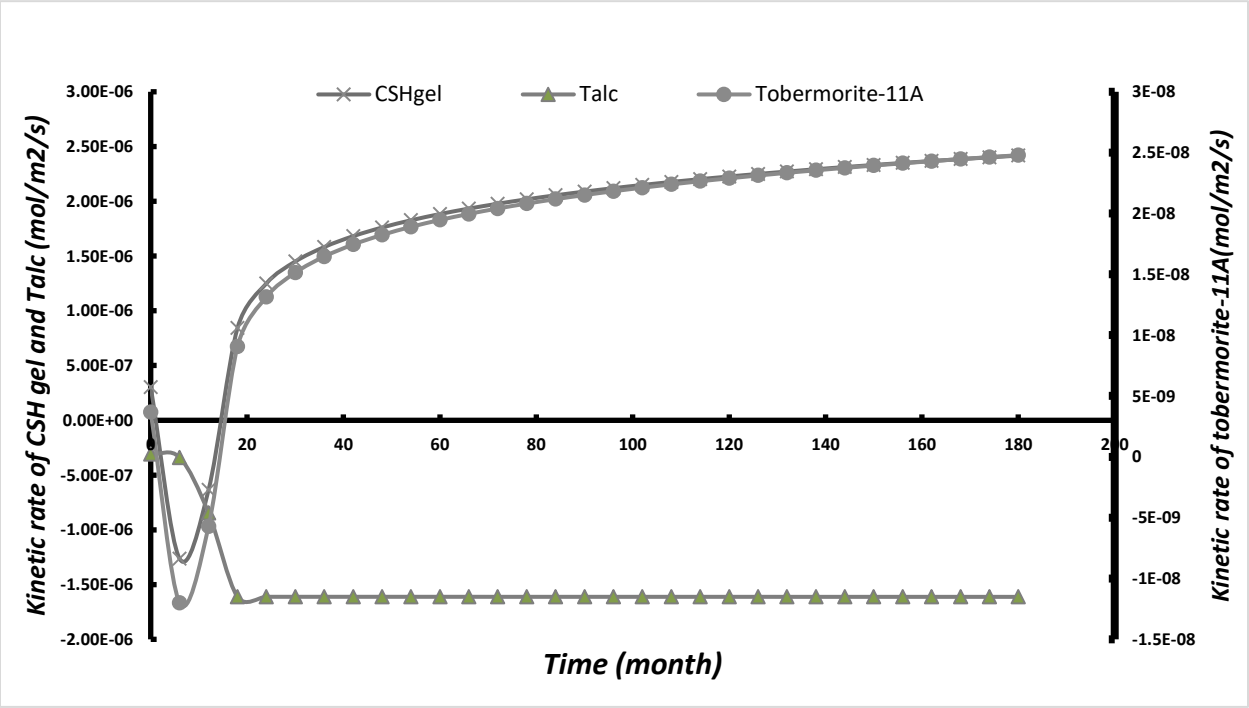

Figure 7: Kinetic rates for CSH gel, talc and tobermorite-11A versus time.

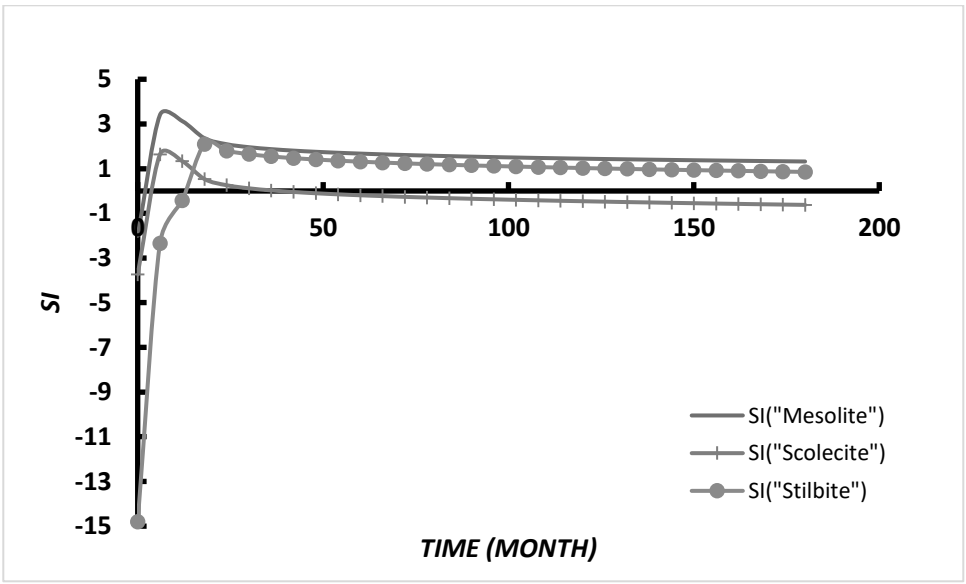

Figure 8: Zeolites minerals saturation indices versus time.

5. Conclusion

The construction of a cement-based, deep underground geological disposal facility for radioactive waste will result in an alkaline plume when groundwater equilibrates with minerals in the cement barrier. This will initiate a series of dissolution/precipitation reactions in the surrounding host rock, and consequent changes in physical, hydraulic, chemical and sorption properties long before any potential migration of radionuclides. It is useful to understand and to be able to predict these changes, as they are likely to influence the potential retardation of future radionuclide migration. This study modelled the mineralogical evolution and geochemical reactions of BVG rock in contact with ENFG. Importantly, the rock sample comprised a hydraulically-conductive dolomite-rich fracture, and though dolomite is only a minor phase in the rock overall, it is a major phase in direct contact with current groundwater. Simulations were conducted using PHREEQC, and predictions compared with data from experiments lasting up to fifteen years. The results showed that: (1) secondary phases such as talc, brucite and Mg-aluminosilicate precipitated, driven by dedolomitization; (2) solution pH initially dropped quickly as a result of brucite precipitation; (3) although zeolites were predicted stable secondary phases, they were absent in the experiments, possibly as a consequence of factors such as slow reaction kinetics, high leachate-to-rock ratios or elevated CO_2 concentrations. Overall, the modelling results of these long-term experiments indicate the important role of fluid-mineral reactions in controlling fluid chemistry and secondary phases, and so sufficient attention should be focused on the mineralogical composition of flowing features, as the minerals lining those can exert a critical influence on key geochemical reactions.

Acknowledgement

The authors acknowledge financial support from NERC in the project *BIogeochemical Gradients and RADionuclide transport* (BIGRAD; Grant Reference NE/H006464/1) for the completion of this work. First and second authors acknowledge Kuwait Petroleum Company (KPC) for sponsoring this work.

References

Adler M, Mäder U, Waber HN (1999) High-pH alteration of argillaceous rocks: an experimental study Schweiz Mineral Petrogr Mitt 79:445-454

Appelo C, Beekman H, Oosterbaan AJIP (1984) Hydrochemistry of springs from dolomite reefs in the southern Alps of northern Italy 150:125-138

Appelo C, Postma DJB, Roterdam (2005) Geochemistry, groundwater and pollution, CRC

Atkinson A, Everitt N, Guppy R (1988) Evolution of pH in a radwaste repository: Internal reactions between concrete constituents. UKAEA Harwell Lab.(UK). Materials Development Div,

Authority ND (2010a) Geological Disposal: Near-field evolution status report. NDA Report NDA/RWMD/033,

Authority ND (2010b) Geological Disposal: Steps Towards Implementation Nuclear Decommissioning Authority Report NDA/RWMD/013

Bateman K, Coombs P, Noy D, Pearce J, Wetton P, Haworth A, Linklater C (1999) Experimental simulation of the alkaline disturbed zone around a cementitious radioactive waste repository: numerical modelling and column experiments Geological Society, London, Special Publications 157:183-194

Berner U (1990) A thermodynamic description of the evolution of pore water chemistry and uranium speciation during the degradation of cement. Paul Scherrer Inst.(PSI),

Bérubé M-A, Choquette M, Locat J (1990) Effects of lime on common soil and rock forming minerals Applied Clay Science 5:145-163

Bethke C (1994) The Geochemist's Workbench, Version 2.0: A Users Guide to Rxn, Act2, Tact, React, and Gtplot. Craig M. Bethke,

Bethke C (1996) Geochemical reaction modeling: Concepts and applications. Oxford University Press on Demand,

Blanc P, Lassin A, Piantone P, Azaroual M, Jacquemet N, Fabbri A, Gaucher EC (2012) Thermoddem: A geochemical database focused on low temperature water/rock interactions and waste materials Applied Geochemistry 27:2107-2116

Braithwaite CJ, Heath RA Alkali–carbonate reactions and 'dedolomitization'in concrete: silica, the elephant in the corner. In, 2013. Geological Society of London,

Braney MC, Haworth A, Jefferies NL, Smith AC (1993) A study of the effects of an alkaline plume from a cementitious repository on geological materials Journal of Contaminant Hydrology 13:379-402 doi:https://doi.org/10.1016/0169-7722(93)90072-Z

Brun A, Engesgaard P (2002) Modelling of transport and biogeochemical processes in pollution plumes: literature review and model development Journal of Hydrology 256:211-227 doi:https://doi.org/10.1016/S0022-1694(01)00547-9

Bucher K, Stober I (2010) Fluids in the upper continental crust Geofluids 10:241-253

549 Bucher K, Weisenberger TB (2013) Fluid-induced mineral composition adjustments during exhumation:
550 the case of Alpine stilbite Contributions to Mineralogy and Petrology 166:1489-1503
551 Chen X, Pao W, Thornton S, Small J (2016) Unsaturated hydro-mechanical–chemical constitutive
552 coupled model based on mixture coupling theory: Hydration swelling and chemical osmosis
553 International Journal of Engineering Science 104:97-109
554 Chen X, Thornton S (2018) Multi-Mineral Reactions Controlling Secondary Phase Evolution in a Hyper-
555 Alkaline Plume Environmental Geotechnics
556 Chen X, Thornton SF, Pao WJIJoES (2018) Mathematical model of coupled dual chemical osmosis based
557 on mixture-coupling theory 129:145-155
558 Chen X, Thornton SF, Small J (2015) Influence of hyper-alkaline pH leachate on mineral and porosity
559 evolution in the chemically disturbed zone developed in the near-field host rock for a nuclear
560 waste repository Transport in Porous Media 107:489-505
561 Cheng K Chemical consumption during alkaline flooding: A comparative evaluation. In: SPE Enhanced
562 Oil Recovery Symposium, 1986. Society of Petroleum Engineers,
563 Choquette M, Berube M-A, Locat J (1991) Behavior of common rock-forming minerals in a strongly
564 basic NaOH solution The Canadian Mineralogist 29:163-173
565 De Windt L, Marsal F, Tinseau E, Pellegrini DJP, Chemistry of the Earth PABC (2008) Reactive
566 transport modeling of geochemical interactions at a concrete/argillite interface, Tournemire site
567 (France) 33:S295-S305
568 Delany J, Lundeen S (1990) The LLNL thermochemical database Lawrence Livermore National
569 Laboratory Report UCRL-21658 150
570 Derkowski A, Bristow TF, Wampler JM, Środoń J, Marynowski L, Elliott WC, Chamberlain CP (2013)
571 Hydrothermal alteration of the Ediacaran Doushantuo Formation in the Yangtze Gorges area
572 (South China) Geochimica et Cosmochimica Acta 107:279-298
573 doi:https://doi.org/10.1016/j.gca.2013.01.015
574 Eglinton M (1998) Resistance of concrete to destructive agencies Lea's chemistry of cement and concrete
575 Fernández R, Rodríguez M, Villa RVdl, Cuevas J (2010) Geochemical constraints on the stability of
576 zeolites and C–S–H in the high pH reaction of bentonite Geochimica et Cosmochimica Acta
577 74:890-906 doi:https://doi.org/10.1016/j.gca.2009.10.042
578 Francis A, Cather R, Crossland IJNSRS, United Kingdon Nirex Limited, 57p (1997) Development of the
579 Nirex Reference Vault Backfill; report on current status in 1994
580 Fridriksson T, Neuhoff P, Bird D, Arnórsson S (1999) Clays and zeolites record alteration history at
581 Teigarhorn, eastern Iceland Geochemistry of the earth's surface Balkema, Rotterdam:377-380
582 Galí S, Ayora C, Alfonso P, Tauler E, Labrador M (2001) Kinetics of dolomite–portlandite reaction:
583 Application to portland cement concrete Cement and Concrete Research 31:933-939
584 doi:https://doi.org/10.1016/S0008-8846(01)00499-9
585 Garcia E, Alfonso P, Tauler E (2020) Mineralogical Characterization of Dolomitic Aggregate Concrete:
586 The Camarasa Dam (Catalonia, Spain) Minerals 10:117
587 Gaucher EC, Blanc P (2006) Cement/clay interactions – A review: Experiments, natural analogues, and
588 modeling Waste Management 26:776-788 doi:https://doi.org/10.1016/j.wasman.2006.01.027
589 Glasser FP (2001) Mineralogical aspects of cement in radioactive waste disposal Mineralogical Magazine
590 65:621-633
591 Harris A, Hearne J, Nickerson A (2001a) The effect of reactive groundwaters on the behaviour of
592 cementitious materials. AEA Technology Report AEAT/R/ENV/0467,
593 Harris A, Manning M, Thompson A (2001b) Testing of models of the dissolution of cements-leaching
594 behaviour of Nirex Reference Vault Backfill. In: AEA Technology Report, AEAT/ERRA-0316.
595 Nirex Ltd. Harwell, UK,
596 Hoch A, Baston G, Glasser F, Hunter F, Smith V (2012) Modelling evolution in the near field of a
597 cementitious repository Mineralogical Magazine 76:3055-3069

598 Hodgkinson ES, Hughes CR (1999) The mineralogy and geochemistry of cement/rock reactions: high-
599 resolution studies of experimental and analogue materials Geological Society, London, Special
600 Publications 157:195-211
601 Kim Y-K et al. (2007) The Korean Final Repository for Low- and Intermediate-Level Radioactive
602 Waste:1383-1387 doi:10.1115/ICEM2007-7130
603 Knauss KGJGeCA (1989) Muscovite dissolution kinetics as a function of pH and time at 70 C 53:1493-
604 1501
605 Lichtner PC (1996) Continuum formulation of multicomponent-multiphase reactive transport Reviews in
606 mineralogy 34:1-82
607 Lothenbach B et al. (2019) Cemdata18: A chemical thermodynamic database for hydrated Portland
608 cements and alkali-activated materials Cement and Concrete Research 115:472-506
609 Mäder UK et al. (2006) Interaction of hyperalkaline fluid with fractured rock: Field and laboratory
610 experiments of the HPF project (Grimsel Test Site, Switzerland) Journal of Geochemical
611 Exploration 90:68-94 doi:https://doi.org/10.1016/j.gexplo.2005.09.006
612 Mayer KU, Frind EO, Blowes DW (2002) Multicomponent reactive transport modeling in variably
613 saturated porous media using a generalized formulation for kinetically controlled reactions Water
614 Resources Research 38:13-11-13-21
615 Min D, Mingshu T (1993) Mechanism of dedolomitization and expansion of dolomitic rocks Cement and
616 Concrete Research 23:1397-1408
617 Moyce EB et al. (2014) Rock alteration in alkaline cement waters over 15 years and its relevance to the
618 geological disposal of nuclear waste 50:91-105
619 Mullis J, Dubessy J, Poty B, O'Neil J (1994) Fluid regimes during late stages of a continental collision:
620 Physical, chemical, and stable isotope measurements of fluid inclusions in fissure quartz from a
621 geotraverse through the Central Alps, Switzerland Geochimica et cosmochimica Acta 58:2239-
622 2267
623 Myers RJ, L'Hôpital E, Provis JL, Lothenbach B (2015) Effect of temperature and aluminium on calcium
624 (alumino) silicate hydrate chemistry under equilibrium conditions Cement and Concrete Research
625 68:83-93
626 Parkhurst DL, Appelo C (1999) User's guide to PHREEQC (Version 2): A computer program for
627 speciation, batch-reaction, one-dimensional transport, and inverse geochemical calculations
628 Pfingsten W, Paris B, Soler JM, Mäder UK (2006) Tracer and reactive transport modelling of the
629 interaction between high-pH fluid and fractured rock: Field and laboratory experiments Journal of
630 Geochemical Exploration 90:95-113
631 Plummer L, Wigley T, Parkhurst DJAjos (1978) The kinetics of calcite dissolution in CO 2-water systems
632 at 5 degrees to 60 degrees C and 0.0 to 1.0 atm CO 2 278:179-216
633 Poole A, Sotiropoulos P (1980) Reactions between dolomitic aggregate and alkali pore fluids in concrete
634 Quarterly Journal of Engineering Geology and Hydrogeology 13:281-287
635 Prommer H, Barry D, Zheng C (2003) MODFLOW/MT3DMS-based reactive multicomponent transport
636 modeling Groundwater 41:247-257
637 Richardson IG (2014) Model structures for c-(a)-sh (i) Acta Crystallographica Section B: Structural
638 Science, Crystal Engineering and Materials 70:903-923
639 Richardson IG, Brough AR, Brydson R, Groves GW, Dobson CM (1993) Location of aluminum in
640 substituted calcium silicate hydrate (C-S-H) gels as determined by 29Si and 27Al NMR and
641 EELS Journal of the American Ceramic Society 76:2285-2288
642 Rimstidt JD, Barnes HJGeCA (1980) The kinetics of silica-water reactions 44:1683-1699
643 Rochelle C, Milodowski A, Bateman K, Moyce E, Hudson-Edwards K (2016) A long-term experimental
644 study of the reactivity of basement rock with highly alkaline cement waters: Reactions over the
645 first 15 months Mineralogical Magazine 80:1089-1113
646 Rochelle C, Pearce J, Bateman K, Coombs P, Wetton P (1997) The Evaluation of Chemical Mass
647 Transfer in the Disturbed Zone of a Deep Geological Disposal Facility for Radioactive Wastes. X,
648 Interaction Between Synthetic Cement Porefluids and BVG: observations from Experiments of 4,

9, and 15 Months Duration: British Geological Survey, Fluid Processes Series, Technical Report WE/97/016.
Savage D et al. (1992) Rate and mechanism of the reaction of silicates with cement pore fluids Applied Clay Science 7:33-45
Savage D, Rochelle CA (1993) Modelling reactions between cement pore fluids and rock: implications for porosity change Journal of Contaminant Hydrology 13:365-378 doi:https://doi.org/10.1016/0169-7722(93)90071-Y
Schwarzenbach EM, Lang SQ, Früh-Green GL, Lilley MD, Bernasconi SM, Méhay S (2013) Sources and cycling of carbon in continental, serpentinite-hosted alkaline springs in the Voltri Massif, Italy Lithos 177:226-244 doi:https://doi.org/10.1016/j.lithos.2013.07.009
Schwyn B, Wersin P, Berner U, Wieland E, Neall F (2003) Near-field chemistry of an ILW repository in Opalinus Clay Unpubl Nagra Internal Rep Nagra, Wettingen, Switzerland
Skogsberg M, Ingvarsson R (2006) Operational experience from SFR-Final repository for low-and intermediate level waste in Sweden.
Small J, Bryan N, Lloyd J, Milodowski A, Shaw S, Morris K (2016) Summary of the BIGRAD project and its implications for a geological disposal facility National Nuclear Laboratory, Report NNL (16) 13817
Soetaert K, Herman PM, Middelburg JJJGeCA (1996) A model of early diagenetic processes from the shelf to abyssal depths 60:1019-1040
Soler JM, Mäder UK (2007) Mineralogical alteration and associated permeability changes induced by a high-pH plume: Modeling of a granite core infiltration experiment Applied Geochemistry 22:17-29 doi:https://doi.org/10.1016/j.apgeochem.2006.07.015
Techer I, Bartier D, Boulvais P, Tinseau E, Suchorski K, Cabrera J, Dauzères A (2012) Tracing interactions between natural argillites and hyper-alkaline fluids from engineered cement paste and concrete: Chemical and isotopic monitoring of a 15-years old deep-disposal analogue Applied Geochemistry 27:1384-1402 doi:https://doi.org/10.1016/j.apgeochem.2011.08.013
Tinseau E, Bartier D, Hassouta L, Devol-Brown I, Stammose D (2006) Mineralogical characterization of the Tournemire argillite after in situ interaction with concretes Waste Management 26:789-800 doi:https://doi.org/10.1016/j.wasman.2006.01.024
Van der Lee J (1997) HYTEC, un modèle couplé hydro-géochimique de migration de polluants et de colloïdes. In: Technical Report LHM/RD/97/02. CIG, École des Mines de Paris Fontainbleau, France,
Van der Lee J (1998) Thermodynamic and mathematical concepts of CHESS
Weisenberger T, Bucher K (2010) Zeolites in fissures of granites and gneisses of the Central Alps Journal of Metamorphic Geology 28:825-847
Weisenberger T, Selbekk RS (2009) Multi-stage zeolite facies mineralization in the Hvalfjördur area, Iceland International Journal of Earth Sciences 98:985-999
Westall J (1986) „Zachary, J. L „Morel, FMM: MINEQL, a computer program for the calculation of the chemical equilibrium composition of aqueous systems. Tech. Note,
Wolery TJ (1992) EQ3/6, a software package for geochemical modeling of aqueous systems: package overview and installation guide (version 7.0)
Wolery TJ, Daveler SA (1992) EQ6, a computer program for reaction path modeling of aqueous geochemical systems: Theoretical manual, users guide, and related documentation (Version 7.0); Part 4. Lawrence Livermore National Lab., CA (United States),
Worley WG (1994) Dissolution kinetics and mechanisms in quartz-and grainite-water systems. Massachusetts Institute of Technology
Xie Q et al. (2013) Mechanism of palygorskite formation in the Red Clay Formation on the Chinese Loess Plateau, northwest China Geoderma 192:39-49 doi:https://doi.org/10.1016/j.geoderma.2012.07.021